A Facile Preparation of Silver Nanocolloids by Hydrogen Reduction of a Silver Alkylcarbamate Complex

Hyun-Ki Hong, Myoung-Seon Gong, and Chan-Kyo Park†,*

Department of Nanobiomedical Science, Dankook University, Chungnam 330-714, Korea
†Department of Applied Chemical Engineering, Dankook University, Chungnam 330-714, Korea
**E-mail: chanpark@dankook.ac.kr*
Received August 11, 2009, Accepted September 25, 2009

Controlled reduction of silver alkylcarbamate complexes with hydrogen gas was investigated as a facile synthetic method for high concentrations of silver nanocolloids in organic solvent. Polyvinylpyrrolidone (PVP) was used to stabilize the silver colloids obtained from the chemical reduction. To determine optimum conditions for preparation of the stable and controlled silver colloids with the narrowest particle size and distribution, a large number of experiments were carried out involving variations in the concentrations of the silver 2-ethylhexylcarbamate (Ag-EHCB) complex, PVP, and 2-propanol. The initial colloid had a mean particle diameter between 5 ~ 50 nm, as measured by transmission electron microscopy, and exhibited a sharp absorption band in the UV region with a maximum size near 420 nm. After treatment with a reducing agent, the colloids were characterized by ultraviolet-visible spectroscopy, X-ray diffraction, and high-resolution transmission electron microscopy.

Key Words: Silver nanocolloid, Silver alkylcarbamate, Reduction, Hydrogen, Organic solvent

Introduction

A variety of methods can be employed for the formation of silver nanoparticles, including electrolysis,[1] biochemical,[2] gas condensation,[3] laser ablation of a silver metal plate,[4] laser irradiation of an aqueous silver solution,[5] sol-gel techniques,[6] sonochemical deposition,[7] nanostructured templates,[8] and thermal decomposition.[9] Generally, silver nanoparticles are synthesized by the reduction of silver salts in the presence of organic stabilizers in a manner similar to the acclaimed Brust's method for the synthesis of gold nanoparticles.[10] The reduction of Ag(I) salt to metallic Ag(0) is carried out by strong reductants such as sodium borohydride,[11,12] sodium citrate,[11,13] hydrogen gas,[14] ascorbic acid,[15,16] DMSO,[17] hydrazine dihydrochloride,[18,19] potassium bitartate,[20] ethanol, pyridine, DMF,[21] and poly (ethylene glycol).[22] However, these reactions have exhibited difficulties in application towards large-scale synthesis in organic solvents owing to their highly diluted and exothermic conditions.

Several silver salt precursors have been employed in the synthesis of silver nanoparticles. Silver nitrate ($AgNO_3$) [11,18,23,24] is the most common source of silver ions, although Ag_2SO_4,[11] silver 2-ethylhexonate,[17] silver oxide,[15] and silver perchlorate[25] have also been used. Generally, the actual size of the nanoparticles obtained varies from system to system, not only because the stabilizer, the reducing agent, and the nature of the metal are varied, but also due to parametrical differences in solvent, concentration, temperature, and reduction time.

Silver organic salts have been used to produce silver nanoparticles and conductive silver tracks. In these processes, silver carboxylate[26-30] or silver alkylcarbamate complexes [31-36] are reduced to silver metal by heating and reduction with hydrazine. However, no other reports have described the formation of silver nanocolloid *via* the one-pot reduction of silver alkylcarbamate complex in organic solution using hydrogen gas as the reducing agent. This method offers the advantages of being able to produce the essentially clean silver particles, which contains no inorganic ions except amine and carbon dioxide, even at room temperature.

The present work examines the preparation of silver nanoparticles through a simple hydrogen reduction process using a silver 2-ethylhexylcarbamate (Ag-EHCB) complex in 2-propanol. The reduction of Ag-EHCB under a hydrogen atmosphere was systematically carried out in order to investigate the effects upon size and morphological characteristics of the silver particles. The experimental conditions, including amount of solvent, concentration of Ag-EHCB and stabilizer for preparation of the silver nanoparticles, and reduction mechanism, were also inferred.

Experimental Section

Chemicals and measurements. The silver 2-ethylhexylcarbamate (Ag-EHCB) complex solution (silver content, 10%) was purchased from Inktec Co. Ltd (Ansan, South Korea). The 2-propanol (Ducksan Chem. Co., Ansan, South Korea) was used as received. The PVP (Aldrich Chem. Co.), molecular weight of 40,000, was used to stabilize the silver colloidal suspensions.

Neither high aspect ratio particles nor any aggregated clusters were removed by gravity-filtration through a membrane filter or centrifugation to concentrate the silver nanoparticle suspension. The TEM observations were carried out using a JEOL electron microscope (JEM-2000EXII). Prior to measurement, the samples were prepared by dropping a small amount of the diluted silver colloid solution to a carbon-coated copper grid. After the solvent evaporated, the particles were sized.

Silver nanocolloid solutions were diluted in 2-propanol and then placed in a quartz cuvette (1 cm path length) with the incident light beam perpendicular to the radial direction of the sam-

Table 1. Conditions for the preparation of silver particles using silver alkylcarbamate complex solution by reduction with hydrogen gas.

Samples (No.)	PVP[a] (g)	Solvent[b] (mL)	Ag-EHCB[c] (g)	[PVP]/[Ag][d]	[Ag-EHCB] × 10^3 (mol/L)	[PVP] × 10^3 (mol/L)
1	1	20	0.05	3.8835	2.3178	9.0
2	1	20	0.1	0.9410	4.6365	9.0
3	1	20	0.2	0.9708	9.2713	9.0
4	1	20	0.3	0.6470	13.9100	9.0
5	1	20	0.4	0.4854	18.5430	9.0
6	1	20	0.5	0.3882	23.1831	9.0
7	1	10	0.1	1.9410	9.2713	9.0
8	1	30	0.1	1.9410	3.0910	9.0
9	1	40	0.1	1.9410	2.3178	9.0
10	0.5	20	0.1	0.9706	4.6365	4.5
11	2	20	0.1	3.8835	4.6365	18.0
12	3	20	0.1	5.8241	4.6365	27.0
13	4	20	0.1	7.7640	4.6365	36.0
14	5	20	0.1	9.7087	4.6365	45.0
15	5	20	0.7	1.3866	32.4560	45.0
16	5	20	0.9	1.0784	41.7290	45.0
17	5	20	1.0	0.9706	46.3650	45.0
18	5	20	1.5	0.6470	69.5480	45.0

[a]Polyvinylpyrrolidone (1 g, 9.0 10^{-3} mol/L); [b]2-Propanol; [c]Silver 2-ethylhexylcarbamate; [d]The ratio of [PVP] to [Ag-EHCB].

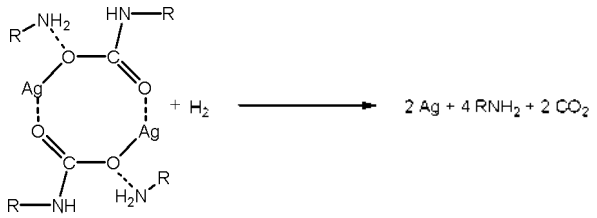

Scheme 1

ple. The UV-Vis spectra were obtained using the Shimadzu UV-1601PC spectrometer over a 200 to 800 nm range with 1 nm resolution and background correction using 2-propanol. The XRD patterns of the Ag nanoparticle were measured using a Shimadzu XD-D1 X-ray diffractometer with CuK_α radiation (λ = 1.54056 Å) at a scanning rate of 2 degrees per second in 2 θ ranging from 30° to 90°. The XRD sample was supported on glass substrates.

Preparation of silver nanocolloid solution. The vessel used for particle synthesis was a 500 mL, stainless steel pressure reactor equipped with a gas regulator and gas inlet and outlet system. The PVP (1.0 g) and silver 2-ethylhexylcarbamate complex (0.10 g) were first dissolved in anhydrous 2-propanol (20.0 g) in the pressure reactor (500 mL). After the reactor was degassed with a vacuum pump, hydrogen gas was pressurized up to 4.5 atm at 25 °C. The solution was then stirred for 2 h to give the silver nanocolloid solution. Other silver nanocolloid solutions with varying PVP content, solvent, and silver carbamate complexes were prepared by similar procedures as described above.

Results and Discussion

Preparation of silver colloidal solution. Silver nanoparticles can be synthesized by the reduction of a silver 2-ethylhexylcarbamate (Ag-EHCB) complex in an organic solvent under a pressurized hydrogen gas atmosphere. Simple charge of the gas over the stirred Ag-EHCB complex solution in 2-propanol at room temperature resulted in formation of a silver colloidal suspension at high concentration. When a solution of the silver carbamate complex reacted with hydrogen, the precursor solution gave the silver metal, carbon dioxide, and a corresponding primary amine as shown in Scheme 1. Because hydrogen and silver alkylcarbamate are the only components used in the reduction, no other inorganic chemical, except an organic amine and carbon dioxide, is present in the final colloidal solution.

This procedure was very efficient and provided the required experimental control for the synthesis of well-defined nanoparticles. Because hydrogen and silver alkylcarbamate were the only components used in the reduction, no other inorganic chemicals were present in the final colloidal solution.

For the dispersion of the produced silver nanoparticles in solution, PVP was employed as the stabilizer. The silver alkylcarbamate complex, in 2-propanol and in the presence of the PVP stabilizer, did not change the color of the solution at the experimental temperature. This result suggested that PVP itself does not reduce the silver alkylcarbamate complex. When hydrogen gas was introduced into the Ag-EHCB complex solution, the solution color changed to a deep brown. At this time, the precursor was rapidly reduced to produce the silver nanoparticles.

To determine the optimum conditions for preparation of stable silver colloids with the narrowest particle size distribution, a large number of experiments were carried out, varying the concentration of Ag-EHCB complex, PVP, and 2-propanol in the reaction mixture, Table 1.

Effect of the concentration of Ag-EHCB. Figure 1 shows a group of UV-Vis absorption spectra for the colloidal solution obtained from 4.6365 × 10^{-3} to 2.3283 × 10^{-2} mol/L of Ag-EHCB complex at the same hydrogen pressure. The complete reduction of the silver colloids could be monitored by UV-Vis spectroscopy, specifically by the appearance of the absorption bands of the

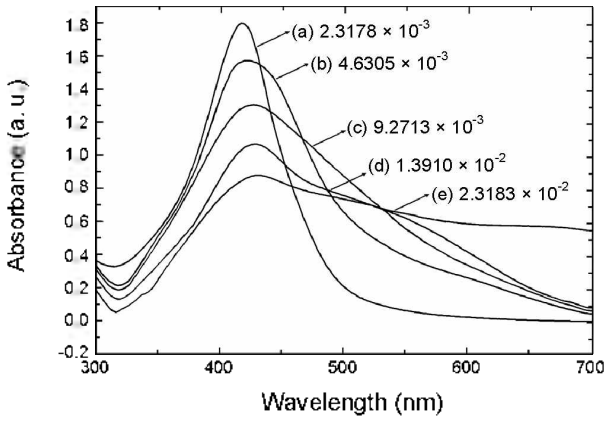

Figure 1. UV-Vis spectra of silver colloidal solutions with different concentration (mol/L) of Ag-EHCB.

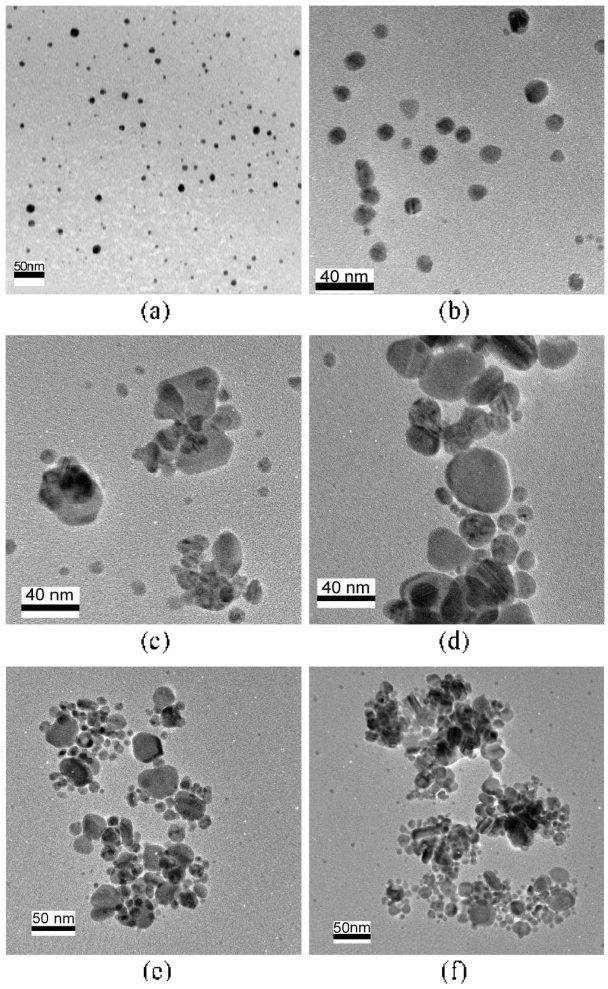

Figure 2. TEM image of different size and shape of silver nanoparticle synthesized by hydrogen reduction of silver alkylcarbamate complex at a concentration of (a) 2.3178×10^{-3}, (b) 4.6365×10^{-3}, (c) 9.2713×10^{-3}, (d) 1.3910×10^{-2}, (e) 1.8543×10^{-2} and (f) 2.183×10^{-2} mol/L.

silver surface plasmon near 420 nm. Because the concentration of Ag-EHCB reached at least 2.3178×10^{-3} mol/L, the maximum UV absorption spectra of the resulting plasmon peak of the silver nanoparticles did not shift below 420 nm. Apparent changes

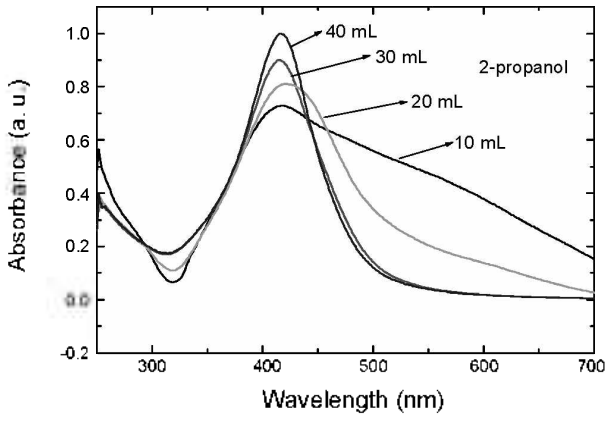

Figure 3. UV-Vis absorption spectra of silver colloidal solutions obtained from various amounts of 2-propanol solvent with 9.0×10^{-3} mol/L of PVP stabilizer.

in absorbance were detected during the two hours under the hydrogen atmosphere at room temperature. Room temperature synthesis of silver nanoparticles was monitored by recording the changes in the UV-Vis spectra over time for different concentrations of the Ag-EHCB complex. At lower Ag-EHCB concentrations, the absorption band was narrowed and shifted continuously to shorter wavelengths as shown in Figure 1(a) and 1(b). In the case of relatively high concentrations of Ag-EHCB (1.8543×10^{-2} and 2.3175×10^{-2} mol/L), a very broad and asymmetric absorbance band was observed, Figure 1(d) and 1(e). Upon increasing the concentration of the Ag-EHCB complex, the band showed a red shift in the maximum of the plasmon peak. These features were associated with the size and distribution of the synthesized silver nanoparticles.

The TEM images of the nanoparticles obtained from six different suspensions are shown in Figure 2. The smallest size (5 ~ 20 nm) shown in Figure 2(a) is from the suspension obtained at a lower Ag-EHCB concentration, 2.3178×10^{-3} and 4.6365×10^{-3} mol/L, while the largest (10 ~ 80 nm) corresponds to higher concentrations obtained from those in experiment No. 3-6 ($|\text{Ag-EHCB}| = 9.2713 \times 10^{-3} \sim 2.3183 \times 10^{-2}$ mol/L). At higher concentrations of Ag-EHCB, the particles were especially multi-dispersing with concomitant aggregation of the particles. At Ag-EHCB concentrations greater than 9.2713×10^{-3} mol/L, agglomerated particles of various sizes and shapes formed en masse, as shown in Fig 2(c)-2(e). In comparison, smaller particles accompanied the agglomerations from Exp No. 3-6, and larger particles without agglomeration for Exp. No. 1 and 2. Most nanoparticles were well-dispersed and sphere-shaped, coinciding with the abovementioned speculation of the UV-Vis absorption spectra.

As a result, a wide distribution of particle sizes have been a distinguishing feature of silver colloids prepared by reduction of silver alkyl carbamate complexes with hydrogen. A variety of shapes from spheres to cubes, and from triangles to hexagons, with lengths of 5 ~ 50 nm and even 80 nm, have been observed in such colloids. These facts are probably due to the inhomogeneity between the Ag-EHCB solution and hydrogen gas in the reaction mixture.

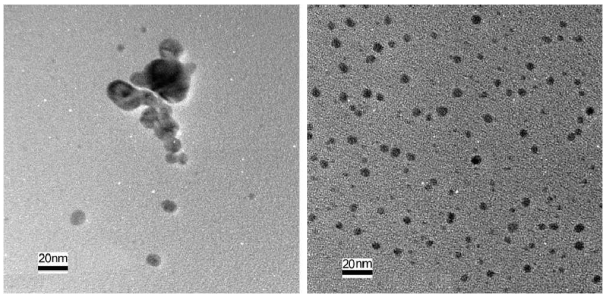

Figure 4. TEM image of silver nanoparticles obtained from Ag-EHCB at a different amount of 2-propanol solvent: Ag-EHCB/2-propanol = (a) 0.1 g/10 mL and (b) 0.1 g/40 mL.

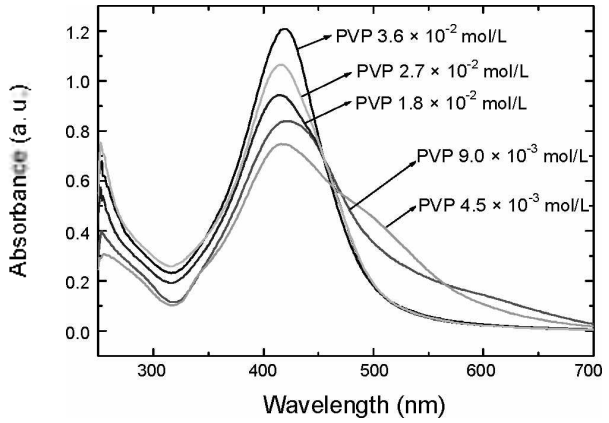

Figure 5. UV-Vis absorption spectra of a PVP protected colloidal solutions.

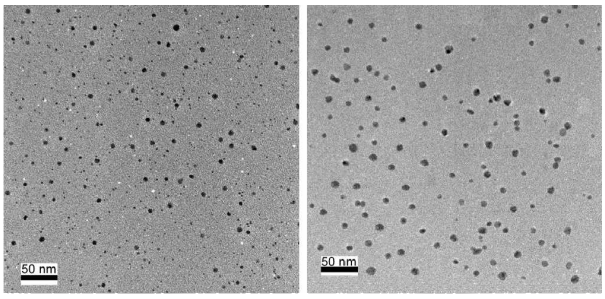

Figure 6. TEM image for the as prepared silver nanoparticles synthesized by hydrogen reduction at a concentration of PVP (a) 2.7×10^{-2} and (b) 3.6×10^{-2} mol/L.

Effect of amount of 2-propanol solvent. An excess of solvent was added to ensure metal atom solvation. Stability turned out to be strongly related with solvent concentration, as with 2-propanol. The more diluted the colloid in 2-propanol, the higher the expected stability. When the amount of 2-propanol was altered, the peak shape and position of the UV absorption spectrum also changed gradually, as shown in Figure 3.

Figure 4 shows TEM micrographs of relatively monodispersed silver particles obtained under different experimental conditions. The final particle size depended on the amount of 2-propanol in the reaction mixture. At higher solvent contents, the primary particles experienced a sufficiently large solvation, which, in combination with the effects of the protected PVP polymer layer, may potentially prevent significant aggregation. Dark brown colloidal silver dispersions were obtained, exhibiting average diameters near 10 or 20 nm. The differences in size are attributed mainly to the varying levels of 2-propanol. In the presence of excess 2-propanol, the growth of stabilized particles ended at a critical size of 5 ~ 10 nm, while the poorly stabilized develop to form larger particles (10 ~ 30 nm) and further agglomerate, Figure 4(a) and 4(b). At lower 2-propanol concentrations, the insufficiency of solvation leads to the vigorous agglomeration and irreversible flocculation observed in Figure 4 (a).

Effect of the concentration of PVP. Figure 5 shows the UV-Vis spectra of silver colloidal solutions under different concentrations of PVP. It can be seen that with an increase in PVP concentration, the full width at the half maximum absorption band due to the silver nanoparticles decreased from 107 to 85 nm, indicating that the particle size distribution became narrower and the colloid system changed from polydispersion to monodispersion upon increase in the concentration of PVP. Note that the strongest intensity and narrowest particle size distribution can be obtained at a minimum concentration of 9.0×10^{-3} mol/L PVP, a very low |PVP|/|Ag| value of 0.9410 due to the existence of regenerated 2-ethylhexylamine during reduction with hydrogen.

When the amount of the stabilizer was insufficient, it could not form a complete protection layer, thus the particles agglomerated easily to form large silver particles. Upon addition of more dispersers, it quickly formed a better-suited layer, protecting the particles from agglomeration and growth, as shown in Exp. No. 10 (|PVP| = 4.5×10^{-3} mol/L). Moreover, upon increasing the ratio of |PVP/Ag-EHCB| from 1.9410 to 9.7087, the band grew more symmetrical and a blue shift in the maximum of plasmon peak appeared. These features were associated with the small and uniform size distribution of the synthesized silver nanoparticles.

For nanoparticles prepared in the presence of a stabilizer, TEM was used for the measurement of nanoparticle size and shape. A typical TEM image for the solution containing a PVP concentration of 2.7×10^{-2} and 3.6×10^{-2} mol/L PVP is shown in Figure 6.

Well-stabilized particles with a critical size near 5 ~ 10 nm formed predominantly under the protection of PVP. Even at higher Ag-EHCB concentrations, the strength of the stabilization was such that less agglomeration occurred and a lower standard deviation was obtained, Figure 6. As for a PVP concentration of 4.5×10^{-2} mol/L, well-stabilized and small particles of 4 ~ 5 nm without agglomeration, resulted. Sufficiently high Ag-EHCB concentrations (15-fold), however, cannot effectively protect the Ag particles so that multidistribution appeared and agglomeration occurred, Figure 7(a)-(c). The average particle size increased with increasing Ag-EHCB concentration, coinciding with the interference from the plasmon absorption spectra.

Stability of silver nanoparticles. To monitor the stability of the final produced silver colloid, the change in time for the absorption spectra of the colloid on different days was measured. There was no obvious change in the shape, position, or asymmetry of the absorption peak during the initial 30 days. The reduction by

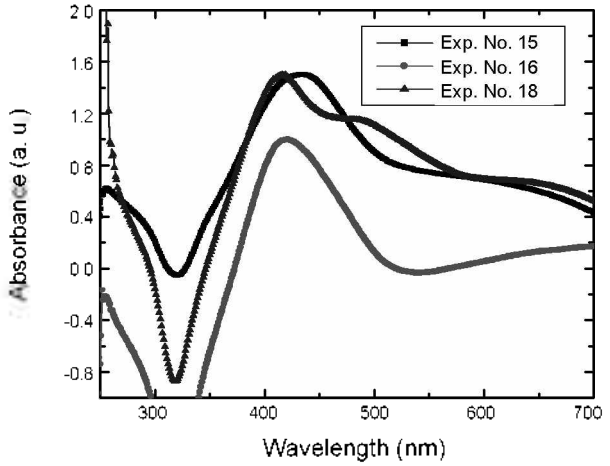

Figure 7. UV-Vis absorption spectra of silver colloidal solutions obtained from various amounts of Ag-EHCB and PVP (a) Exp. No. 15, (b) Exp. No. 16 and (c) Exp. No. 18.

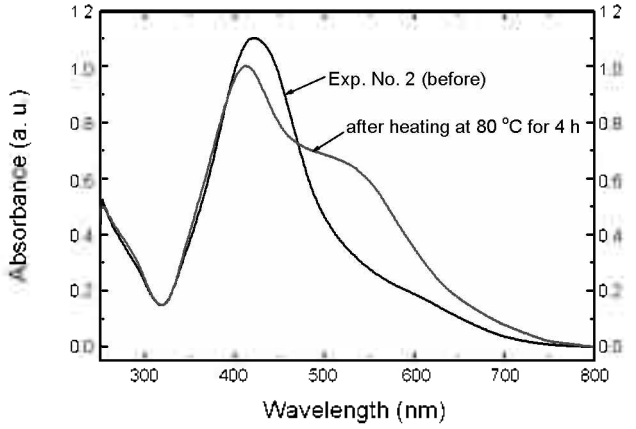

Figure 8. UV-Vis absorption spectra of silver colloidal solutions obtained from colloidal solution a) before and b) after heating for 4 hr at 80 °C.

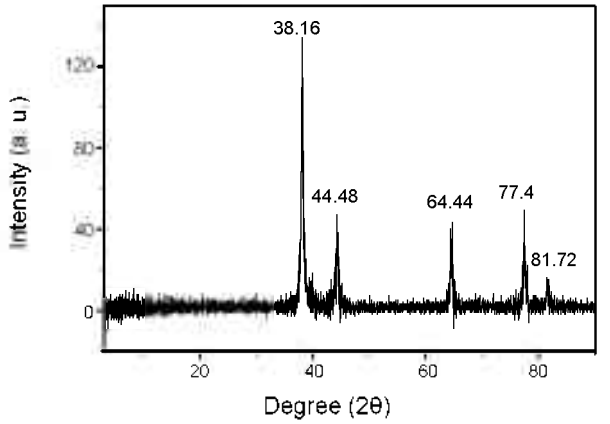

Figure 9. Powder X-ray diffraction pattern of a silver nanoparticle obtained from silver colloid solution (Exp. No. 15).

hydrogen resulted in very stable samples without precipitation occurring after 30 days or months. When the colloidal solution from Exp. No. 2 was heated at 80 °C for 24 h, the full width of highest maxima (fwhm) of the spectrum grew wider than before, and the peak maximum and shape showed a red shift with asymmetry, implying the onset of nanoparticle aggregation.

Characterization. The nanoparticles synthesized by hydrogen reduction were characterized with XRD. The XRD pattern of the silver nanoparticles with a diameter 5 ~ 50 nm obtained from a 2-propanol solution suspension at a concentration of 2.183×10^{-2} mol/L is shown in Figure 9. The pattern exhibits peaks at 2 θ angles of 38.16, 44.48, 64.44, 77.40, and 81.72 that correspond to the (111), (200), (220), (311), and (222) crystal planes of silver, respectively.

Conclusion

In conclusion, colloidal silver particles in the nanosize range were prepared in 2-propanol by the reduction of silver 2-ethylhexylcarbamate complex with hydrogen. The main mechanism is the hydrogen reduction of the silver carbamate complex to the neutral state of silver by hydrogen. Furthermore, we can point out that the use of a silver alkylcarbamate complex solution on silver/PVP dispersions can be employed to obtain silver dispersions in organic solvents such as 2-propanol, a method unique from others described in the literature. As such, a facile method for the preparation of silver nanocolloid dispersions containing no inorganic ions was developed using a silver carbamate complex.

Acknowledgments. The present research was conducted by the research fund of Dankook University in 2009.

References

1. Rodriguez-Sanchez, L.; Blanco, M. C.; Lopez-Quintela, M. A. *J. Phys. Chem. B* **2000**, *104*, 9683.
2. Mukherjee, P.; Ahmad, A.; Mandal, D.; Senapati, S.; Sainkar, S. R.; Khan, M. I.; Parishcha, R.; Ajaykumar, P. V.; Alam, M.; Kumar, R.; Sastry, M. *Nano Lett.* **2001**, *1*, 515.
3. Hayashi, T.; Ohno, T.; Yatsuya, S.; Uyeda, R. *Jpn. J. Appl. Phys.* **977**, *16*, 705.
4. Mafune, F.; Kohno, J.; Takeda, Y.; Kondow, T. *J. Phys. Chem. B* **2000**, *104*, 8333.
5. Abid, J. P.; Wark, A. W.; Brevet, P. F.; Girault, H. H. *Chem. Commun.* **2002**, 792.
6. Brugger, P. A.; Guendet, P.; Gratzel, M. *J. Am. Chem. Soc.* **1981**, *103*, 2923.
7. Pol, V. G.; Srivastava, D. N.; Palchik, O.; Palchik, V.; Slifkin, M. A.; Weiss, A. M.; Gedanken, A. *Langmuir* **2002**, *18*, 3352.
8. Dai, J.; Bruening, M. L.; *Nano Lett.* **2002**, *2*, 497.
9. Manna, A.; Imae, T.; Iida, M.; Hisamatsu, N. *Langmuir* **2001**, *17*, 6000.
10. Brust, M.; Walker, M.; Bethell, D.; Schiffrin, D. J.; Whyman, R. *J. Chem. Soc. Chem. Commun.* **1994**, 801.
11. Lee, P. C.; Meisel, D. *J. Phys. Chem.* **1982**, *86*, 3391.
12. Creighton, J. A.; Blatchford, C. G.; Albrecht, M. G. *J. Chem. Soc. Faraday Trans.* **1979**, *275*, 790.
13. Turkevich, J.; Stevenson, P. C.; Hiller, J. *Discuss. Faraday Soc.* **1951**, *11*, 55-75.
14. Evanoff, Jr., D. D.; Chumanov, G. *J. Phys. Chem. B* **2004**, *108*, 13948.
15. Sondi, I.; Matijević, D. V. E. *J. Colloid Interface Sci.* **2003**, *260*, 75.
16. Velikov, K. P.; Zegeres, G. E.; van Blaaderen, A. *Langmuir* **2003**, *19*, 1384.

17. Rodríguez-Gattorno, G.; Díaz, D.; Rendoń, L.; Hernández-Segura, G. O. *J. Phys. Chem. B* **2002**, *106*, 2482.
18. Nickel, U.; Castell, A.; Pöppl, K.; Shirtcliffe, N. *Langmuir* **2000**, *16*, 9087.
19. Leopold, N.; Lendl, B. J. *Phys. Chem. B* **2003**, *107*, 5723.
20. Tan, Y.; Dai, X.; Li, Y.; Zhu, D. *J. Mater. Chem.* **2003**, *13*, 1069.
21. He, R.; Qian, X.; Yin, J.; Zhu, Z. *J. Mater. Chem.* **2002**, *12*, 3783.
22. Chen, D. H.; Huang, Y. W. *J. Colloid Interface Sci.* **2002**, *255*, 299.
23. Nie, S.; Emory, S. R. *Science* **1997**, *275*, 1102.
24. Shirtcliffe, N.; Nickel, U.; Schneider, S. *J. Colloid Interface Sci.* **1999**, *211*, 122.
25. Van Hyning, D. L.; Zukoski, C. F. *Langmuir* **1998**, *14*, 7034.
26. Kashiwagi, Y.; Yamamoto, M.; Nakamoto, M. *J. Colloid Interface Sci.* **2006**, *300*, 169.
27. Szymańska, I.; Piszczek, P.; Szczęsny, R.; Szlyk, E. *Polyhedron* **2007**, *26*, 2440.
28. Liu, X.; Luc, S.; Zhang, J.; Cao, W. *Thermochimica Acta* **2006**, *440*, 1.
29. Monti, O. L. A.; Fourkas, J. T.; Nesbitt, D. J. *J. Phys. Chem. B* **2004**, *108*, 1604.
30. Singh, N.; Khanna, P. K. *Mater. Chem. Phys.* **2007**, *104*, 367.
31. Park, M. S.; Lim, T. H.; Jeon, Y. M.; Kim, J. G.; Joo, S. W.; Gong, M. S. *Macromol. Res.* **2008**, *16*, 308.
32. Park, M. S.; Lim, T. H.; Jeon, Y. M.; Kim, J. G.; Joo, S. W.; Gong, M. S. *Sens. Actuators B* **2008**, *133*, 166.
33. Grodzicki, A.; Lakomska, I.; Piszczek, P.; Szymańska, I.; Szlyk, E. *Coord. Chem. Rev.* **2005**, *249*, 2232.
34. Park, M. S.; Lim, T. H.; Jeon, Y. M.; Kim, J. G.; Joo, S. W.; Gong, M. S. *J. Colloid Interface Sci.* **2008**, *321*, 60.
35. Jeon, Y. M.; Cho, H. N.; Gong, M. S. *Macromol. Res.* **2009**, *17*, 2.
36. Lim, T. H.; Jeon, Y. M.; Gong, M. S. *Polymer(Korea)* **2009**, *33*, 33.